

Unveiling Passive and Active EMF Exposure in Large-Scale Cellular Networks

Yujie Qin, Mustafa A. Kishk, *Member, IEEE*, Ahmed Elzanaty, *Senior Member, IEEE*, Luca Chiaraviglio, *Senior Member, IEEE*, and Mohamed-Slim Alouini, *Fellow, IEEE*

Abstract—With the development of fifth-generation (5G) networks, the number of user equipments (UE) increases dramatically. However, the potential health risks from electromagnetic fields (EMF) tend to be a public concern. Generally, EMF exposure-related analysis mainly considers the passive exposure from base stations (BSs) and active exposure that results from the user’s personal devices while communicating. However, the passive radiation that is generated by nearby devices of other users is typically ignored. In fact, with the increase in the density of UE, their passive exposure to human bodies can no longer be ignored. In this work, we propose a stochastic geometry framework to analyze the EMF exposure from active and passive radiation sources. In particular, considering a typical user, we account for their exposure to EMF from BSs, their own UE, and other UE. We derive the distribution of the Exposure index (EI) and the coverage probability for two typical models for spatial distributions of UE, i.e., *i*) a Poisson point process (PPP); *ii*) a Matern cluster process. Also, we show the trade-off between the EMF exposure and the coverage probability. Our numerical results suggest that the passive exposure from other users is non-negligible compared to the exposure from BSs when user density is 10^2 times higher than BS density, and non-negligible compared to active exposure from the user’s own UE when user density is 10^5 times the BS density.

Index Terms—Electric and magnetic fields exposure; uplink transmission; Poisson point process; Matern cluster process; passive and active exposure.

I. INTRODUCTION

The fifth-generation of cellular networks (5G) has been designed to guarantee low delays and high throughput, accommodate high user density, meet the goal of wide coverage, and connect the unconnected regions [1], [2]. In fact, the number of mobile users has increased from 3.6 billion to 5.2 billion from 2014 to 2020 [3]. Despite much research effort and advanced communication techniques that have been accomplished to design rate and energy-efficient networks, developing networks with reduced electromagnetic field (EMF) exposure is still an open problem that concerns the public [4].

Yujie Qin and Mohamed-Slim Alouini are with Computer, Electrical and Mathematical Sciences and Engineering (CEMSE) Division, King Abdullah University of Science and Technology (KAUST), Thuwal, 23955-6900, Saudi Arabia (e-mail: yujie.qin@kaust.edu.sa; slim.alouini@kaust.edu.sa).

Mustafa Kishk is with the Department of Electronic Engineering, Maynooth University, Maynooth, W23 F2H6, Ireland (e-mail: mustafa.kishk@mu.ie).

A. Elzanaty is with the 5GIC & 6GIC, Institute for Communication Systems (ICS), University of Surrey, Guildford, GU2 7XH, United Kingdom (e-mail: a.elzanaty@surrey.ac.uk).

L. Chiaraviglio is with the Department of Electronic Engineering, Università degli Studi di Roma Tor Vergata, 00133 Rome, Italy and Consorzio Nazionale Interuniversitario per le Telecomunicazioni (CNIT), Parma, Italy (e-mail: luca.chiaraviglio@uniroma2.it).

Generally, EMF exposure is classified as passive and active exposure, in which passive exposure is commonly composed of exposure from base stations (BSs) and active exposure resulting from the user’s personal devices. Based on the guidelines provided by International Telecommunication Union (ITU) [5], International Commission on Non-Ionizing Radiation Protection (ICNIRP) [6], and Federal Communications Commission (FCC) [7], each country has its regulations regarding the safety limits for EMF exposure and some restrictions on BSs deployment [8]. These guidelines and regulations are mainly developed to guarantee that the temperature elevation of the exposed tissues is within a safe limit [9], [10].

Surprisingly, most of the concerns about EMF exposure are from the deployment of BSs, even if the emissions from mobile phones present a significant component as the UE antennas are much closer to the human body [11]. In this regard, it is a fundamental task to guarantee that the EMF exposure from all the components (e.g., BS and UE) in future networks is below the acceptable safe levels [12], [13].

Motivated by the aforementioned importance of designing EMF-efficient networks and considering the exponential growth in the number of UE, in this work, we propose a stochastic geometry framework to analyze the EMF exposure of the whole network. In particular, considering a typical user, we account for their exposure to EMF from BSs, their own UE, and other UE. Specifically, we use tools from stochastic geometry to model the locations of UE and BSs and study the passive and active exposure.

A. Related Work

Literature related to this work can be categorized into: (i) experimental EMF exposure assessment, (ii) analytical EMF exposure assessment and design. A brief discussion on related works in each of these categories is discussed in the following lines.

EMF exposure experimental assessment. Authors in [14] investigated the EMF exposure in 5G systems compared to the EMF exposure measured in previous generations. Authors in [15] measured the EMF from a BS by using an integrated approach and performing a large set of measurements over the territory. A spectrum analyzer-based measurement methodology was proposed in [16] to evaluate the time-averaged instantaneous exposure. Some other approaches to assess 5G EMF exposure were provided in [17], [18]. For instance, authors in [17] analyzed the EMF for commercial 5G

networks but considered transmit power monitoring of a set of 5G BSs. Authors in [18] pointed out the need for dynamic monitoring of EMF exposure and proposed a dynamic measurement approach for carrying out rapid extensive monitoring of radio-frequency EMF which can be used to characterize the dynamics of EMF in 5G systems.

Analytical EMF exposure assessment and design. For EMF-aware cellular system design, a resource allocation scheme was developed in [19] to minimize the EMF exposure. Rate-splitting multiple access (RSMA)-based with EMF constraints was investigated in [20] where the uplink energy efficiency is enhanced while limiting the EMF exposure under a certain level. A reconfigurable intelligent surface (RIS)-assisted network was analyzed in [21] to minimize the EMF exposure of users while maintaining a minimum target quality of service. In addition, authors in [22] proposed to maximize the minimum SINR in RIS networks while limiting the EMF exposure of users considering statistical channel state information (CSI).

For analytical EMF assessment, authors in [23] presented a statistical model, which is based on modeling the expectation of the statistically conservative fraction of the total power contributing to the EMF exposure within an arbitrary beam, to estimate the time-averaged realistic maximum power levels for the assessment of EMF exposure using massive MIMO. In [24], authors proposed another statistic model, which is based on a three-dimensional spatial channel model, for modeling the 5G EMF exposure of massive MIMO systems. As for the effect of massive MIMO on the EMF exposure, authors in [25] revealed that the pencil beamforming may be beneficial for the network throughput and reducing the EMF level. A novel approach was proposed in [26] for EMF analysis by comparing the radio BS EMF and EMF generated by 5G smartphones.

While previous related works only analyze the EMF exposure from a relatively small number of BSs, large-scale network EMF analysis is essential for 5G network design. In [27], the problem of 5G BS locations planning under EMF exposure limits is considered. A stochastic geometry approach to EMF exposure modeling was proposed in [28] and the author validated the model using experimental data. Manhattan Poisson line process (MPLP) was used in [29] to derive the joint distributions of data rate and EMF exposure. A stochastic geometry-based analysis was used in [30] and authors analyzed the impact of the network parameters and discussed the trade-off between coverage and EMF exposure. Besides, a stochastic geometry-based analysis of EMF in sub-6 GHz and mmWave networks was proposed in [31], in which the locations of mmWave BSs and sub-6 GHz BSs are modeled by Poisson point processes (PPPs). In [32], Poisson hole process is used to capture the impact of having restricted areas where BSs are not allowed to be deployed. Next, the downlink, uplink, and joint downlink & uplink exposure induced by the radiation from BSs and personal UE are analyzed.

Different from the existing literature, which mainly neglects the EMF exposure from active uplink users, our work analyzes the total exposure from all network components including the passive EMF exposure from active uplink users. More details on the contributions of this paper are provided next.

B. Contributions

This paper investigates the EMF exposure of a network composed of BSs and UEs. Different from existing literature, which only focuses on the impact of the EMF passive exposure from BSs and active exposure from the user's personal equipment, we capture the passive exposure which is composed of all active uplink users and BSs. We study the impact of system parameters such as user density, uplink path-loss compensation factor, and the number of antennas on the EMF exposure. The main contributions of this work are summarized as follows.

- We propose a stochastic geometry-based framework to study the EMF exposure of two types of users: (i) passive users and (ii) active users, in which the passive user does not participate in the communication process (not using UE), and the active user participates in uplink communication. In particular, we consider the exposure from all sources, both BSs and active uplink UE.
- In order to capture the scenario of spatially-clustered UE, which is commonly found in different use cases such as in airports or schools we model the locations of UE using MCP. To the best of the authors' knowledge, this is the first work to address the influence of UE spatial-clustering on EMF exposure. The inhomogeneity in the spatial distribution of UE in the case of MCP introduces some mathematical challenges, specially in computing total passive uplink EMF exposure, which we carefully handle in this paper. We also provide the analysis in the case of PPP to establish meaningful comparisons.
- Using tools from stochastic geometry, we are able to compute the mean and cumulative density function (CDF) of exposure index (EI, which is a performance metric to characterize the level of EMF exposure formally defined in Definition 6) under PPP and MCP models, respectively.

II. SYSTEM MODEL

We are interested in studying the impact of user distributions, user densities, BS density, and uplink transmission on EMF exposure. In this regard, we consider a wireless cellular network where the locations of BSs are modeled by a PPP, denoted by Φ_b with density λ_b , we consider two types of user distributions, PPP and MCP, respectively [33]–[35]. In this work, we compute the EMF exposure considering two types of users: (i) a passive user and (ii) an active user (active uplink user), defined below.

Definition 1 (Passive User). *Passive user denotes a user who is not an uplink user. Therefore, the EMF exposure of the passive user is composed of the exposure from (i) all BSs, due to the downlink transmission between BSs and users, and (ii) all active uplink users. Besides, we assume that the passive user is located at the origin (stationarity of PPP [36]).*

Definition 2 (Active User). *Active user denotes an active uplink user. Therefore, the EMF exposure of the active user is composed of the exposure from (i) all BSs, (ii) all other active uplink users, and (iii) its uplink transmission. Without loss of generality, we randomly select one active uplink user as our reference user.*

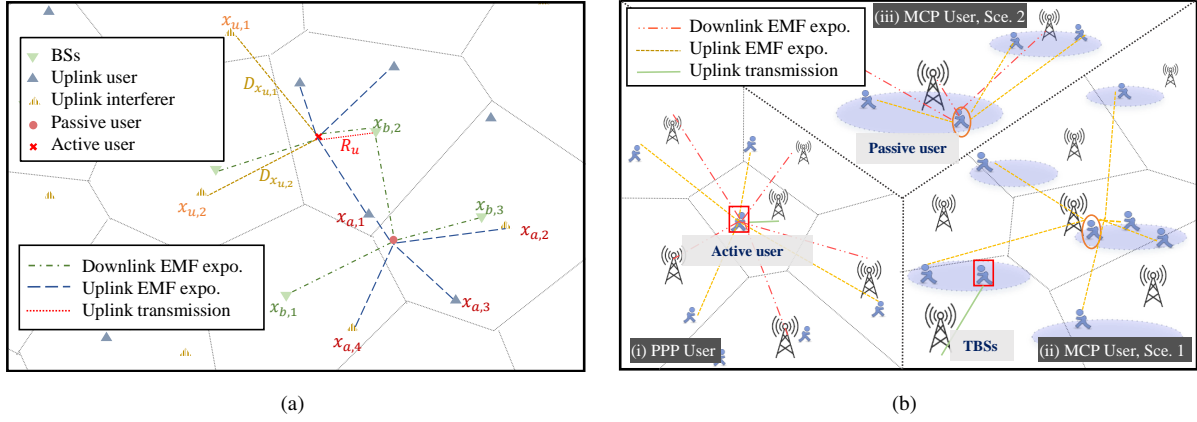


Fig. 1. Illustration of system model: (a) Passive and active user, and (b-i) PPP user, (b-ii) MCP user, Scenario 1, and (b-iii) MCP user, Scenario 2.

TABLE I
TABLE OF NOTATIONS

Notation	Description
Φ_b, Φ_u	Point set of the locations of BSs, locations of PPP users
x_b, x_u, x_a	Locations of BSs, locations of interfering uplink users, locations of active uplink users
$R_u, D_{\{ \cdot \}}$	Distance to the serving BS, distance between two locations
Φ_c, Φ_{cu}	Locations of user cluster centers, locations of MCP users
$\lambda_b, \lambda_u, \lambda_c, \lambda_{cu}$	Density of BSs, density of PPP users, density of user clusters, density of users in a cluster
$\Phi_{ue}, \Phi'_{ue}, \Phi'_{ue}$	Locations of all uplink users, locations of active uplink users, locations of interfering uplink users
η, α, β	Power inversion control factor, path-loss of communication, path-loss of exposure
ρ_b, ρ_u, p_{max}	Transmit power of BSs, minimum transmit power of UEs, maximum transmit power of UEs
$W_b, W_{b,a}$	EMF exposure from BSs (passive user, PPP user model), EMF exposure from BSs (active user, PPP user model)
$W'_b, W'_{b,a}$	EMF exposure from BSs (passive user, MCP user model), EMF exposure from BSs (active user, MCP user model)
$W_u, W_{u,\{1,2\}}$	EMF exposure from uplink users (PPP user model), EMF exposure from uplink users (MCP user model, passive user, Sec. 1 & 2)
$W_{u,a,\{1,2\}}$	EMF exposure from uplink users (MCP user model, active user, Sec. 1 & 2)
SAR_{ul}, SAR_{dl}	Reference induced SAR in uplink, Reference induced SAR in downlink
$El_p, El_{p,\{1,2\}}, El_a$	Exposure Index (passive user, PPP user model), Exposure Index (MCP users, Sec. 1 & 2), Exposure Index (active user)
$El_{bs}, El_{ul}, El_{ul,tr}$	Exposure Index of BSs, Exposure Index of active uplink users, Exposure Index of the uplink transmission of active user
P_{cov}, I, σ^2	Coverage probability, interference, noise power

The system model is shown in Fig. 1 and related notations are explained in Table I and the definitions below.

Definition 3 (PPP User model). *At places where users are scattered uniformly on the whole plane, we model the locations of users by a PPP denoted by Φ_u with density λ_u .*

Definition 4 (MCP User model). *At places where users are spatially clustered, we model the locations of users by a MCP. Particularly, we consider two scenarios: Scenario 1: the locations of user cluster centers are independent to BSs and modeled by a PPP, denoted by Φ_c , with density λ_c , and Scenario 2: user clusters are centered at BSs, which means that users are scattered around the BSs. For both scenarios, users are uniformly distributed in the user clusters with radius r_c , and let Φ_{cu} denote the locations of all cluster users, and λ_{cu} denote the user density of a user cluster.*

To simplify the notations, we use Φ_{ue} to present the locations of all uplink users, e.g., in the case of PPP user model $\Phi_{ue} = \Phi_u$ and in the case of MCP user model $\Phi_{ue} = \Phi_{cu}$. Let Φ'_{ue} denote the locations of the active uplink users which is obtained from an independent thinning of Φ_u with an active probability p_a [36].

In the uplink transmission, users associate with their nearest BSs and the association regions of the users with the BSs form

a Poisson-Voronoi (PV) tessellation [37], [38]. In addition, we assume that the BSs allocate the resources to avoid inter-cell interference. Hence, from the perspective of a certain resource block and a certain PV cell, only one uplink user is active and the interfering users can only be from other cells. Let Φ''_{ue} be the locations of the interfering users for the uplink transmission; hence, Φ''_{ue} is a subset of Φ'_{ue} . However, all active uplink users contribute to EMF exposure regardless of their different resource blocks and association cells.

A. Communication Model

We first introduce the communication model of the considered system. We consider BSs equip with omnidirectional antenna with antenna gain G_b , and for the uplink transmission, the received power at the BS is given by

$$p_r = G_b p_u H R_u^{-\alpha}, \quad (1)$$

in which the variable H models the small-scale Rayleigh fading of the channel and follows the exponential distribution with a mean of unity. We assume that the inversion power control technology considered in [39] is adopted. From [39], for a given $R_u = r_u$, the truncated transmission power of a user is given by

$$p_u = \begin{cases} \rho_u r_u^\alpha \eta, & 1 \leq r_u < r_0, \\ p_{max}, & r_u \geq r_0, \end{cases} \quad (2)$$

in which r_u denotes the distance between the user and the serving BS, ρ_u is the minimum transmit power for the adopted uplink power control technique, α is the path-loss for calculating SINR and η is the path-loss compensation factor, p_{\max} denotes the maximum transmit power of a mobile user, and $r_0 = (p_{\max}/\rho_u)^{1/\alpha\eta}$.

Recall that we randomly select one active uplink user as our reference user and its serving BS as tagged BS. Generally, coverage probability is defined as the probability that the reference user is successfully served, which denotes the event that the SINR of the related link is above a predefined threshold.

Definition 5 (Uplink Coverage Probability). *The uplink coverage probability is defined as*

$$P_{\text{cov}}(\gamma) = \mathbb{P}(\text{SINR} > \gamma), \quad (3)$$

in which SINR denotes the signal-to-interference-plus-noise ratio at the serving BS, I is the aggregate interference, and γ is the required SINR threshold,

$$\text{SINR} = \frac{p_r}{\sigma^2 + I}, \quad I = \sum_{x \in \Phi''_{\text{ue}}} p_{u,x} H_x D_x^{-\alpha}, \quad (4)$$

in which σ^2 is the normalized uplink transmission noise power: $\sigma^2 = \frac{\sigma_r'^2}{l_u}$, l_u the path-loss at the reference distance $d_0 = 1$ m, $l_u = (\frac{c}{4\pi d_0})^2$ and σ^2 is the noise power, $p_{u,x}$ denotes the transmit power, H_x denotes the channel fading of user $x \in \Phi''_{\text{ue}}$, and D_x is the distance between the user x_u and the tagged BS.

B. EMF Exposure

EI is the performance metric defined to characterize individual exposure and it is built from the aggregation of exposure from different sources and situations. In the proposed system, the exposure sources are composed of BSs and active uplink users and the personal mobile of the active user. To compute the EI of the passive user and the active user, we first analyze the EMF exposure from the aforementioned sources.

Let p_b and p_o be the received power from a BS and UE, respectively,

$$p_b(D_x) = \rho_b G_b H_x D_x^{-\beta}, \quad p_o(D_x) = p_{u,x} H_x D_x^{-\beta},$$

where ρ_b is the transmit power of the BSs, $D_{\{\cdot\}}$, $H_{\{\cdot\}}$ present the distance and channel fading, respectively, and β denotes the EMF path-loss, where $\beta > 2$ is assumed to guarantee the convergence of the integration. Consequently, the incident power densities from BSs and other UEs¹, W_b and W_u , are respectively given by

$$\begin{aligned} W_b &= \sum_{x \in \Phi_b} \frac{\rho_b G_b H_x}{4\pi} D_x^{-\beta}, \\ W_u &= \sum_{x \in \Phi'_{\text{ue}}} \frac{p_{u,x} H_x}{4\pi} D_x^{-\beta}, \end{aligned} \quad (5)$$

where $p_{u,x}$ is the truncated transmit power for the user located at x , $x \in \Phi_b$. Recall that the EMF exposure of the passive user

¹Note that when we analyze the W_u for the active user defined in Def. 2, Φ'_{ue} denotes the locations of other active UEs except the one we analyze.

is composed of the exposure from all BSs and all active uplink users and the EMF exposure of the active user is composed of the exposure from all BSs, other active uplink users, and its uplink transmission. Therefore, the EI of the passive user and active user is formally defined as follows.

Definition 6 (Exposure Index). *The EI EI_p of the passive user is defined as*

$$EI_p = EI_{\text{bs}} + EI_{\text{ul,u}}, \quad (6)$$

in which EI_{bs} and $EI_{\text{ul,u}}$ are the EI of BSs and active uplink users, respectively, and given by

$$EI_{\text{bs}} = \text{SAR}_{\text{dl}} W_b, \quad EI_{\text{ul,u}} = \text{SAR}_{\text{dl}} W_u,$$

where SAR_{dl} is the reference induced SAR in downlink when the received power density from BSs is unitary.

Similarly, the EI of the active user is defined as

$$EI_a = EI_{\text{bs}} + EI_{\text{ul,u}} + EI_{\text{ul,tr}}, \quad (7)$$

in which $EI_{\text{ul,tr}}$ is the EI of uplink transmission of the active user

$$EI_{\text{ul,tr}} = \text{SAR}_{\text{ul}} p_u,$$

where SAR_{ul} is the reference induced SAR in uplink when the transmit power from user equipment is unity, respectively.

III. EI ANALYSIS OF PPP USER MODEL

In this section, we provide the analysis of EI in the case that users are PPP distributed. To do so, we first compute the PDF of the transmit power and then obtain the Laplace transform of W_b and W_u , respectively. Since the truncated path-loss inversion power control is used, the transmit power is a mixed random variable and its PDF is given in the following lemma.

Lemma 1 (Distribution of the Transmit Power). *The PDF of p_u is given by*

$$\begin{aligned} f_{p_u}(p) &= \frac{2\pi\lambda_b}{\alpha\eta\rho_u^{\alpha\eta}} p^{\frac{2}{\alpha\eta}-1} \exp\left(-\pi\lambda_b\left(\frac{p}{\rho_u}\right)^{\frac{2}{\alpha\eta}}\right) \\ &+ \exp\left(-\pi\lambda_b\left(\frac{p_{\max}}{\rho_u}\right)^{\frac{2}{\alpha\eta}}\right) \delta_{p_{\max}}(p), \quad \rho_u < p \leq p_{\max}, \end{aligned} \quad (8)$$

in which $\delta_{p_{\max}}(p)$ is an impulse at p_{\max} and satisfies $\int_0^\infty \delta_{p_{\max}}(p) dp = 1$.

Proof: This Lemma follows by using the PDF of the contact distance of a PPP. ■

It is difficult to compute the CDF of EI_p and EI_a directly. Alternatively, we can use the Gil-Pelaez theorem which requires the characteristic function or Laplace transform of EI_p and EI_a . Hence, in the following lemma, we first derive the Laplace transform of the W_b and W_u , then the Laplace transform of EI_p and EI_a can be obtained by the multiplication of the Laplace transform of W_b and W_u .

1) *Passive User:* We first compute the Laplace transform of W_b and W_u for the passive user. Recall that the passive user is located at the origin, and the passive EMF exposure includes the exposure from all BSs and active uplink users.

Lemma 2 (Laplace Transform of W_u and W_b of the Passive User). *For the passive user, the Laplace transform of W_u and W_b is given by*

$$\mathcal{L}_{W_u}(s) = \exp\left(-2\pi\lambda_u p_a \int_0^\infty \int_{\rho_u}^{p_{\max}} \left(\frac{f_{p_u}(x)}{1+4\pi(sx)^{-1}z^\beta}\right) dx dz\right),$$

$$\mathcal{L}_{W_b}(s) = \exp\left(-\lambda_b \int_0^\infty \left(\frac{1}{1+4\pi(s\rho_b G_b)^{-1}z^\beta}\right) z dz\right).$$

Proof: The Laplace transform of W_u is given by

$$\mathcal{L}_{W_u}(s) = \mathbb{E}_{\Phi'_u, H, p_u} \left[\prod_{x \in \Phi'_u} \exp\left(-s \frac{p_u H \|x\|^{-\beta}}{4\pi}\right) \right]$$

$$\stackrel{(a)}{=} \mathbb{E}_{\Phi'_u, p_u} \left[\prod_{x \in \Phi'_u} \left(\frac{1}{1+sp_u \|x\|^{-\beta} (4\pi)^{-1}}\right) \right]$$

$$\stackrel{(b)}{=} \exp\left(-2\pi\lambda_u p_a \int_0^\infty \int_{\rho_u}^{p_{\max}} \left[1 - \left(\frac{1}{1+spz^{-\beta} (4\pi)^{-1}}\right)\right] f_{p_u}(p) dp z dz\right), \quad (9)$$

in which step (a) follows from using the MGF of exponential random variable and step (b) follows from using PGFL of PPP. The Laplace transform of W_b follows similar steps, thus omitted here. ■

Lemma 3 (Laplace Transform of EI_p). *The Laplace transform of EI_p is given by*

$$\mathcal{L}_{EI_p}(s) = \mathcal{L}_{W_b}(s \text{ SAR}_{\text{dl}}) \mathcal{L}_{W_u}(s \text{ SAR}_{\text{dl}}), \quad (10)$$

in which $\mathcal{L}_{W_b}(s)$, $\mathcal{L}_{W_u}(s)$ are obtained in Lemma 2.

Proof: The Laplace transform of EI_p is computed by

$$\mathcal{L}_{EI_p}(s) = \mathbb{E}_{EI_p}[\exp(-s EI_p)]$$

$$= \mathbb{E}_{W_u, W_b} \left[\exp\left(-s \text{ SAR}_{\text{dl}}(W_b + W_u)\right) \right]$$

$$\stackrel{(a)}{\approx} \mathbb{E}_{W_u} \left[\exp\left(-s \text{ SAR}_{\text{dl}} W_u\right) \right] \mathbb{E}_{W_b} \left[\exp\left(-s \text{ SAR}_{\text{dl}} W_b\right) \right] \quad (11)$$

in which step (a) follows from assuming W_b and W_u to be independent (note that this is an approximation² that shows good matching as evident in the numerical results section). The proof completes by substituting the Laplace transform of W_u and W_b . ■

Consequently, by using the Gil-Pelaez theorem [40], the CDF and mean of EI_p are given in the following theorem.

Theorem 1 (CDF and Mean of EI_p). *The CDF and mean of the total passive exposure, including exposure from BSs and active uplink users are, respectively, given by*

$$F_{EI_p}(w) = \frac{1}{2} - \frac{1}{2j\pi} \int_0^\infty \frac{1}{t} [\exp(-jtw) \mathcal{L}_{EI_p}(-jt) - \exp(jtw) \mathcal{L}_{EI_p}(jt)] dt, \quad (12)$$

$$\bar{EI}_p = \text{SAR}_{\text{dl}} \frac{\lambda_u p_a}{2(\beta-2)} \bar{p}_{u,p} + \text{SAR}_{\text{dl}} \frac{\rho_b G_b \lambda_b}{2(\beta-2)}, \quad (13)$$

²Note that the random variables W_b and W_u are generally not independent given that the adopted uplink power control technique makes the transmit powers of the users function of the locations of the BSs.

in which j is the imaginary unit, $\bar{p}_{u,p} = \int_0^\infty \max(p_{\max}, \rho_u r^{\eta\alpha}) f_{R_u}(r) dr$ is the mean of uplink transmit power, where $f_{R_u}(r) = 2\lambda_b \pi r \exp(-\pi\lambda_b r^2)$ is the PDF of PPP contact distance.

Proof: From Gil-Pelaez theorem [40], the CDF has the following relation with the characteristic function,

$$F_{EI_p}(w) = \frac{1}{2} - \frac{1}{\pi} \int_0^\infty \frac{1}{t} \Im(\exp(-jtw) \phi_{EI_p}(t)) dt$$

$$= \frac{1}{2} - \frac{1}{2\pi} \int_0^\infty \frac{1}{jt} (\exp(-jtw) \phi_{EI_p}(t) - \exp(jtw) \phi_{EI_p}(-t)) dt, \quad (14)$$

in which $\Im(\cdot)$ denotes the imaginary part of a complex number, and proof completes by substituting $\mathcal{L}_{EI_p}(-jt) = \phi_{EI_p}(t)$.

The mean of EI_p is given by

$$\mathbb{E}[EI_p] = \text{SAR}_{\text{dl}} (\mathbb{E}[W_u] + \mathbb{E}[W_b]), \quad (15)$$

in which

$$\mathbb{E}[W_u] = \left. \frac{\partial M_{W_u}(s)}{\partial s} \right|_{s=0} = \left. \frac{\partial \mathcal{L}_{W_u}(-s)}{\partial s} \right|_{s=0}$$

$$= \frac{2\pi\lambda_u p_a}{4\pi} \int_0^\infty \int_0^\infty \min(p_{\max}, \rho_u r^{\alpha\eta}) z^{-\beta+1} f_{R_u}(r) dr dz$$

$$= \frac{\lambda_u p_a}{2(\beta-2)} \int_0^\infty \min(p_{\max}, \rho_u r^{\alpha\eta}) f_{R_u}(r) dr, \quad (16)$$

$$\mathbb{E}[W_b] = \left. \frac{\partial \mathcal{L}_{W_b}(-s)}{\partial s} \right|_{s=0} = 2\pi\lambda_b G_b \int_0^\infty \rho_b (4\pi)^{-1} z^{-\beta+1} dz$$

$$= \rho_b G_b (4\pi)^{-1} \frac{2\pi\lambda_b}{(\beta-2)}. \quad (17)$$

2) *Active User:* In the case of computing the EI of the active user, while the Laplace transform of W_u of the active user the same as the passive user, the EMF exposure from BSs is correlated with the exposure from the uplink transmission of the active user, e.g., the distance to the nearest BS is the same as the distance considered while computing the uplink transmit power. Hence, in order to compute the Laplace transform of the total exposure of the active user, we need to compute the Laplace transform for each of the downlink exposure and the uplink self-exposure conditioned on the distance to the serving BS before taking the expectation over this distance.

Hence, the Laplace transform of downlink exposure for active users, $W_{b,a}$ (except the exposure from the nearest BS, which is $W_{b,0}$ and will be introduced later in the text), is computed as a function of the communication distance between the active user and its serving BS.

Lemma 4 (Laplace Transform of $W_{b,a}$ of the Active User). *For the active user, the Laplace transform of $W_{b,a}$ is given by*

$$\mathcal{L}_{W_{b,a}}(s, R_u) = \exp\left(-\lambda_b \int_{R_u}^\infty \left(\frac{z^{-\beta+1}}{1+4\pi(s\rho_b G_b)^{-1}}\right) dz\right).$$

Consequently, the Laplace transform of EI_a , composed of the exposure from (i) the nearest BS, (ii) remaining BSs, (iii) active uplink users, and (iv) uplink transmission of the active user, is given in the following lemma.

Lemma 5 (Laplace Transform of EI_a). *The Laplace transform of EI_a conditioned on R_u is given by*

$$\mathcal{L}_{EI_a}(s, R_u) = \mathcal{L}_{W_{b,a}}(s \text{ SAR}_{\text{dl}}, R_u) \mathcal{L}_{W_u}(s \text{ SAR}_{\text{dl}})$$

$$\begin{aligned} & \times \exp\left(-s \text{SAR}_{\text{ul}} \min(p_{\max}, \rho_{\text{u}} R_{\text{u}}^{\alpha_{\text{u}}})\right) \\ & \times \left(\frac{1}{1 + s \text{SAR}_{\text{dl}} \rho_{\text{b}} G_{\text{b}} R_{\text{u}}^{-\beta} (4\pi)^{-1}}\right). \end{aligned} \quad (18)$$

In the following theorem, we provide the CDF of EI_{a} as well as the mean of EI_{a} .

Theorem 2 (CDF and Mean of EI_{a}). *The CDF of the total exposure, including exposure from BSs, active uplink users and the uplink transmission of the active user, is given by*

$$F_{\text{EI}_{\text{a}}}(w) = \frac{1}{2} - \frac{1}{2j\pi} \int_0^{\infty} \int_0^{\infty} \frac{1}{t} [\exp(-jtw) \mathcal{L}_{\text{EI}_{\text{a}}}(-jt, r) - \exp(jtw) \mathcal{L}_{\text{EI}_{\text{a}}}(jt, r)] f_{R_{\text{u}}}(r) dr dt,$$

in which $f_{R_{\text{u}}}(r) = 2\pi r \lambda_{\text{b}} \exp(-\pi r^2)$.

The mean of EI_{a} is given by

$$\begin{aligned} \bar{\text{EI}}_{\text{a}} &= \int_0^{\infty} \left(\text{SAR}_{\text{dl}} (4\pi)^{-1} \left(G_{\text{b}} \rho_{\text{b}} r^{-\beta} + \frac{2\pi \lambda_{\text{b}} G_{\text{b}} \rho_{\text{b}}}{\beta - 2} r^{2-\beta} \right) \right. \\ & \quad + \text{SAR}_{\text{ul}} \min(p_{\max}, \rho_{\text{u}} r^{\alpha_{\text{u}}}) \left. \right) f_{R_{\text{u}}}(r) dr \\ & \quad + \text{SAR}_{\text{dl}} \frac{\lambda_{\text{u}} p_{\text{a}}}{2(\beta - 2)} \bar{p}_{\text{u}, p}, \end{aligned} \quad (19)$$

recall that $f_{R_{\text{u}}}(r) = 2\pi r \lambda_{\text{b}} \exp(-\pi \lambda_{\text{b}} r^2)$.

Proof: Similar to the passive user case, the CDF of EI_{a} can be obtained from the Laplace transform using Gil-Pelaez theorem [40].

For the mean of EI_{a} , recall that EI_{a} is composed of the exposure from (i) nearest BS, (ii) remaining BSs, (iii) active uplink users, and (iv) uplink transmission of the active user, in which (i), (iii) and (iv) are functions of the communication distance R_{u} . Therefore, the mean is given by

$$\mathbb{E}[\text{EI}_{\text{a}}] = \mathbb{E}[\text{SAR}_{\text{dl}} W_{\text{u}}] + \mathbb{E}[\text{SAR}_{\text{dl}}(W_{\text{b}, \text{a}} + W_{\text{b}, 0}) + \text{SAR}_{\text{ul}} p_{\text{u}}],$$

in which

$$\begin{aligned} \mathbb{E}[\text{SAR}_{\text{dl}} W_{\text{u}}] &= \text{SAR}_{\text{dl}} \mathbb{E} \left[\sum_{x \in \Phi'_{\text{ue}}} \frac{p_{\text{u}, x} H_x}{4\pi} D_x^{-\beta} \right] \\ &\stackrel{(a)}{=} \frac{\text{SAR}_{\text{dl}}}{4\pi} \mathbb{E} \left[\sum_{x \in \Phi'_{\text{ue}}} p_{\text{u}, x} D_x^{-\beta} \right] \\ &= \frac{\text{SAR}_{\text{dl}}}{4\pi} \mathbb{E} \left[\sum_{x \in \Phi'_{\text{ue}}} \min(p_{\max}, \rho_{\text{u}} R_{\text{u}}^{\alpha_{\text{u}}}) D_x^{-\beta} \right] \\ &\stackrel{(b)}{=} \frac{\lambda_{\text{u}} \text{SAR}_{\text{dl}}}{2} \int_0^{\infty} \frac{1}{z^{\beta}} z dz \int_0^{\infty} \min(p_{\max}, \rho_{\text{u}} r^{\alpha_{\text{u}}}) f_{R_{\text{u}}}(r) dr \\ &= \text{SAR}_{\text{dl}} \frac{\lambda_{\text{u}} p_{\text{a}}}{2(\beta - 2)} \int_0^{\infty} \min(p_{\max}, \rho_{\text{u}} r^{\alpha_{\text{u}}}) f_{R_{\text{u}}}(r) dr \\ &\stackrel{(c)}{=} \text{SAR}_{\text{dl}} \frac{\lambda_{\text{u}} p_{\text{a}}}{2(\beta - 2)} \bar{p}_{\text{u}, p}, \end{aligned} \quad (20)$$

where step (a) follows from the fact that all channel fading coefficients are independent and exponentially distributed random variables with unity mean, (similar to [41, Lemma 2] and [42]), step (b) follows from Campbell's theorem [36] with the conversion from Cartesian to polar coordinates and the independence of $p_{\text{u}, x}$ and D_x , and step (c) follows from the definition of $\bar{p}_{\text{u}, p}$ given in the proof of Theorem 1,

$$\mathbb{E}[\text{SAR}_{\text{dl}}(W_{\text{b}, \text{a}} + W_{\text{b}, 0}) + \text{SAR}_{\text{ul}} \frac{H p_{\text{u}}}{4\pi}]$$

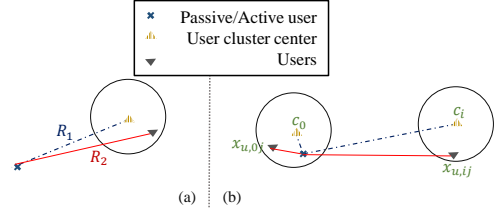


Fig. 2. Illustration of (a) conditional distance: the relation between R_1 and R_2 , and (b) MCP system model: the locations of user cluster centers and users.

$$\begin{aligned} &= \mathbb{E}_{R_{\text{u}}} \left[\text{SAR}_{\text{dl}} \mathbb{E} \left[\sum_{x \in \Phi_{\text{b}} \setminus x_{b_0}} \frac{\rho_{\text{b}} G_{\text{b}} H_x}{4\pi} D_x^{-\beta} \right] \right. \\ & \quad + \text{SAR}_{\text{dl}} \mathbb{E} \left[\frac{\rho_{\text{b}} G_{\text{b}} H_{x_{b_0}}}{4\pi} R_{\text{u}}^{-\beta} \right] + \frac{\text{SAR}_{\text{ul}} H}{4\pi} \min(p_{\max}, \rho_{\text{u}} R_{\text{u}}^{\alpha_{\text{u}}}) \left. \right] \\ &= \mathbb{E}_{R_{\text{u}}} \left[\text{SAR}_{\text{dl}} \frac{\lambda_{\text{b}} G_{\text{b}} \rho_{\text{b}}}{2(\beta - 2)} R_{\text{u}}^{2-\beta} \right. \\ & \quad \left. + \text{SAR}_{\text{dl}} \frac{\rho_{\text{b}} G_{\text{b}}}{4\pi} R_{\text{u}}^{-\beta} + \frac{\text{SAR}_{\text{ul}}}{4\pi} \min(p_{\max}, \rho_{\text{u}} R_{\text{u}}^{\alpha_{\text{u}}}) \right], \end{aligned} \quad (21)$$

in which x_{b_0} denotes the location of the serving BS, b_0 is the serving BS, and the proof completes by integrating over R_{u} . ■

IV. EI ANALYSIS OF MCP USER MODEL

In this section, we provide the analysis of EI when the users are spatially clustered. To do so, we first compute the PDF of the distance between the reference user and an active uplink user from any cluster. Next, we obtain the Laplace transform of W_{b} and W_{u} . Conditioning on the distance to the cluster center R_1 , the distribution of the distance to the user in the cluster R_2 , as shown in Fig. 2 (a), is given in the following lemma.

Lemma 6 (Distance Distribution). *Conditioned on the user cluster center being located at a distance R_1 from the user, the PDF of the distance to an active uplink user is given as in [35] as follows. For $R_1 < r_c$, we have*

$$f_{R_2}(r_2|R_1) = \begin{cases} \frac{2r_2}{r_c^2}, & 0 \leq r_2 \leq r_c - R_1, \\ \frac{2r_2}{\pi r_c^2} \arccos\left(\frac{r_2^2 + R_1^2 - r_c^2}{2r_2 R_1}\right), & r_c - R_1 \leq r_2 \leq r_c + R_1, \end{cases}$$

while for $R_1 > r_c$, we have

$$f_{R_2}(r_2|R_1) = \frac{2r_2}{\pi r_c^2} \arccos\left(\frac{r_2^2 + R_1^2 - r_c^2}{2r_2 R_1}\right), \quad R_1 - r_c \leq r_2 \leq r_c + R_1, \quad (22)$$

and $f_{R_2}(r_2|R_1) = 0$, otherwise.

In what follows, we compute the Laplace transform of W_{u} . Note that in the case of MCP user model with PPP distributed BSs (Scenario 1), the Laplace transform of W_{b} and $W_{\text{b}, \text{a}}$ are the same as the PPP user model since they are independent of the cluster centers. On the other hand, if BSs are located at the cluster centers (Scenario 2) $W'_{\text{b}} = W_{\text{b}} + W_{\text{b}, \text{c}}$ and $W'_{\text{b}, \text{a}} = W_{\text{b}, \text{a}} + W_{\text{b}, \text{c}}$, where $W_{\text{b}, \text{c}}$ denotes the exposure of

BS located at the reference user's cluster center. To compute the Laplace transform of W_u , we first define the cluster point process.

A system illustration is shown in Fig. 2 (b). Let Φ_c be the location of user cluster centers, modeled by a PPP with density λ_c . With each point $c_i \in \Phi_c$, associate with a point process $\Phi_{c_i,u}$. The point process Φ_c is generally called the parent process and $\Phi_{c_i,u}$ is called the offspring process. The union of offspring points processes is termed a cluster point process, denoted by $\Phi_{cu} = \cup_{c_i \in \Phi_c} c_i + \Phi_{c_i,u}$. In the case that the points in each point process, $x_{c_i,u_j} \in \Phi_{c_i,u}$, are uniformly distributed in the ball with radius r_c and center c_i , $B(c_i, r_c)$, Φ_{cu} is so-called Matern cluster process (MCP). Consequently, the locations of each point in MCP are given by

$$\Phi_{cu} = \left\{ x_{u,ij} : c_i + x_{c_i,u_j}, c_i \in \Phi_c, x_{c_i,u_j} \in \Phi_{c_i,u}, \{i, j\} \in \mathbb{N} \right\}. \quad (23)$$

Besides, conditioned on the passive user located at the origin and the passive user's cluster contains the origin, the Palm distribution of the mentioned MCP is given by $\Phi_{cu}^0 = \Phi_{cu} \cup \{x_{u,0j}\}$ in which $\{x_{u,0j} : c_0 + x_{c_0,u_j}, (0, 0) \in B(c_0, r_c), x_{c_0,u_j} \in \Phi_{c_0,u}, j \in \mathbb{N}\}$. Similarly, let p_a be the active probability of the uplink user and Φ_{cu}' be the point set of the locations of the active uplink users. Recall that in the MCP user case, we consider two scenarios: Scenario 1: the locations of user clusters are independent of the locations of BSs, and Scenario 2: user clusters are centered at BSs. In Scenario 1, we assume that the active uplink users from the same cluster have the same transmit power (due to the relative small variance of transmit powers among users within the same cluster) and each user associates with its nearest BS. In Scenario 2, we assume that the user associates with the BS deployed at the cluster center.

1) *Passive User*: The Laplace transform of $W_{u,\{1,2\}}$ of the passive user, in which the subscript $\{1, 2\}$ denotes Scenario 1 and Scenario 2, respectively, is given in the following lemma.

Lemma 7 (Laplace Transform of W_u , Scenario 1 & 2). *In Scenario 1, the Laplace transform of W_u of the passive user is given by*

$$\begin{aligned} \mathcal{L}_{W_{u,1}}(s) &\approx \exp \left\{ -2\pi\lambda_c \int_0^\infty 1 - \int_0^\infty \exp \left(-p_a\lambda_{cu}\pi r_c^2 \right. \right. \\ &\times \left. \int_0^{r_c+r_1} \frac{f_{R_2}(r|r_1)}{1+(sp(z))^{-1}(4\pi)r^\beta} dr \right) f_{R_u}(z) dz r_1 dr_1 \left. \right\} \\ &\times \int_0^{r_c} \exp \left(-p_a\lambda_{cu}\pi r_c^2 \int_0^{r_c+r_1} \frac{f_{R_2}(r|r_1)}{1+(sp(z))^{-1}(4\pi)r^\beta} dr \right) \\ &\times f_{R_u}(z) dz \frac{2r_1}{r_c^2} dr_1, \end{aligned} \quad (24)$$

in which $p(z) = \min(p_{\max}, \rho_u z^{\alpha\eta})$.

In Scenario 2, the Laplace transform of W_u of the passive user is given by

$$\begin{aligned} \mathcal{L}_{W_{u,2}}(s) &\approx \exp \left\{ -2\pi\lambda_c \int_0^\infty 1 - \exp \left(-p_a\lambda_{cu}\pi r_c^2 \int_0^{r_c+r_1} \right. \right. \\ &\left. \left. \frac{f_{R_2}(r|r_1)}{1+(s\bar{p}_{u,m})^{-1}(4\pi)r^\beta} dr \right) r_1 dr_1 \right\} \int_0^{r_c} \int_0^\infty \exp \left(-p_a\lambda_{cu}\pi r_c^2 \right. \end{aligned}$$

$$\left. \int_0^{r_c+r_1} \frac{f_{R_2}(r|r_1)}{1+(s\bar{p}_{u,m})^{-1}(4\pi)r^\beta} dr \right) \frac{2r_1}{r_c^2} dr_1, \quad (25)$$

in which $\bar{p}_{u,m} = \int_0^{r_c} \min(p_{\max}, \rho_u z^{\alpha\eta}) \frac{2z}{r_c^2} dz$.

Proof: See Appendix A. ■

Similar to the PPP user model, we compute the CDF and mean of EI_p , which are given in the following theorem.

Theorem 3 (CDF and Mean of EI_p , Scenario 1 & 2). *The CDF of the total passive exposure, including exposure from BSs and active uplink users is given by*

$$\begin{aligned} F_{EI_{p,1}}(w) &= \frac{1}{2} - \frac{1}{2j\pi} \int_0^\infty \frac{1}{t} [\exp(-jtw)\mathcal{L}_{EI_{p,1}}(-jt) \\ &\quad - \exp(jtw)\mathcal{L}_{EI_{p,1}}(jt)] dt, \\ F_{EI_{p,2}}(w) &= \frac{1}{2} - \frac{1}{2j\pi} \int_0^\infty \int_0^{r_c} \frac{1}{t} [\exp(-jtw)\mathcal{L}_{EI_{p,2}}(-jt) \\ &\quad - \exp(jtw)\mathcal{L}_{EI_{p,2}}(jt)] f_{R'_u}(r) dr dt, \end{aligned}$$

in which

$$\begin{aligned} \mathcal{L}_{EI_{p,\{1,2\}}}(s) &= \mathcal{L}_{\{W_b, W'_b\}}(s \text{ SAR}_{dl}) \mathcal{L}_{W_{u,\{1,2\}}}(s \text{ SAR}_{dl}), \\ \mathcal{L}_{W'_b}(s) &= \mathcal{L}_{W_b}(s \text{ SAR}_{dl}) \exp \left(-s \text{ SAR}_{dl} \frac{\rho_b G_b}{4\pi} R_u^{-\beta} \right), \end{aligned} \quad (26)$$

and R'_u has the PDF $f_{R'_u}(r) = \frac{2r}{r_c^2}$.

The mean of the total passive exposure, including exposure from BSs and active uplink users is given by

$$\begin{aligned} \bar{E}I_{p,1} &= \text{SAR}_{dl} \frac{\bar{p}_{u,p} \lambda_c p_a \lambda_{cu} \pi r_c^2}{2} \int_0^\infty \int_0^{r_c+r_1} r^{-\beta} f_{R_2}(r|r_1) dr r_1 dr_1 \\ &+ \text{SAR}_{dl} \frac{\bar{p}_{u,p} p_a \lambda_{cu} r_c^2}{4} \int_0^{r_c} \int_0^{r_c+r_1} r^{-\beta} f_{R_2}(r|r_1) dr \frac{2r_1}{r_c^2} dr_1 \\ &+ \text{SAR}_{dl} \rho_b \frac{\lambda_b G_b}{2(\beta-2)}, \\ \bar{E}I_{p,2} &= \text{SAR}_{dl} \frac{\bar{p}_{u,m} \lambda_c p_a \lambda_{cu} \pi r_c^2}{2} \int_0^\infty \int_0^{r_c+r_1} r^{-\beta} f_{R_2}(r|r_1) dr r_1 dr_1 \\ &+ \text{SAR}_{dl} \rho_b \frac{\lambda_b G_b}{\pi(\beta-2)} + \frac{\text{SAR}_{dl}}{4\pi} \int_0^{r_c} \left(\rho_b G_b r_1^{-\beta} + \right. \\ &\left. \frac{\bar{p}_{u,m} p_a \lambda_{cu} \pi r_c^2}{2} \int_0^{r_c+r_1} r^{-\beta} f_{R_2}(r|r_1) dr \right) \frac{2r_1}{r_c^2} dr_1. \end{aligned} \quad (27)$$

Proof: Follows a similar way as PPP user model, thus omitted here. ■

2) *Active user*: Compared to the Laplace transform of W_u of PPP user model, as well as the passive user case, the Laplace transform of W_u in the case of MCP user model is slightly different. This is because of the number of active intra-cluster uplink users: the total number of active uplink users in the same cluster is a Poisson random variable with parameter $n \sim \text{Exp}(p_a \lambda_{cu} \pi r_c^2)$, the intra-cluster EMF exposure W_{u,c_0} is from all the cluster users except the active user. With that being said, $W_{u,c_0} = \sum_{k=0}^{n-1} \frac{p_{u,x_k} H_{x_k}}{4\pi} D_{x_k}^{-\beta}$. The Laplace transform of $W_{u,a,\{1,2\}}$ of the active user is given in the following lemma.

Lemma 8 (Laplace Transform of $W_{u,a,\{1,2\}}$, Scenario 1 & 2). *In Scenario 1, the Laplace transform of $W_{u,a,1}$ of the active user is given by*

$$\begin{aligned} \mathcal{L}_{W_{u,a,1}}(s) &\approx \exp \left\{ -2\pi\lambda_c \int_0^\infty 1 - \int_0^\infty \exp \left(-p_a\lambda_{cu}\pi r_c^2 \right. \right. \\ &\left. \left. \int_0^{r_c+r_1} \frac{f_{R_2}(r|r_1)}{1+(sp(z))^{-1}(4\pi)r^\beta} dr \right) f_{R_u}(z) dz r_1 dr_1 \right\} \end{aligned}$$

$$\times \int_0^{r_c} \int_0^\infty \frac{\exp(-p_a \lambda_{cu} \pi r_c^2)}{\int_0^{r_c+r_1} \frac{f_{R_2}(r|R_u)}{1+s\bar{p}(z)(4\pi)^{-1}r^{-\beta}} dr} \left(\exp\left(p_a \lambda_{cu} \pi r_c^2\right) \int_0^{r_c+r_1} \frac{f_{R_2}(r|R_u)}{1+s\bar{p}(z)(4\pi)^{-1}r^{-\beta}} dr \right) - 1 \Big) f_{R_u}(z) dz \frac{2r_1}{r_c^2} dr_1. \quad (28)$$

In Scenario 2, the Laplace transform of W_u of the passive user is given by

$$\mathcal{L}_{W_{u,a,2}}(s) \approx \exp\left\{-2\pi\lambda_c \int_0^\infty 1 - \exp\left(-p_a \lambda_{cu} \pi r_c^2 \int_0^{r_c+r_1} \frac{f_{R_2}(r|R_u)}{1+(s\bar{p}_{u,m})^{-1}(4\pi)r^\beta} dr\right) r_1 dr_1\right\} \int_0^{r_c} \frac{\exp(-p_a \lambda_{cu} \pi r_c^2)}{\int_0^{r_c+r_1} \frac{f_{R_2}(r|R_u)}{1+s\bar{p}_{u,m}(4\pi)^{-1}r^{-\beta}} dr} \left(\exp\left(p_a \lambda_{cu} \pi r_c^2 \int_0^{r_c+r_1} \frac{f_{R_2}(r|R_u)}{1+s\bar{p}_{u,m}(4\pi)^{-1}r^{-\beta}} dr\right) - 1 \right) \frac{2r_1}{r_c^2} dr_1. \quad (29)$$

Proof: See Appendix B. ■

Obtained the Laplace transform of $W_{u,a,\{1,2\}}$, we are able to derive the CDF and mean of EI_a , which are given in the following two theorems.

Theorem 4 (CDF and Mean of EI_a , Scenario 1 & 2). *The CDF of the total passive exposure, including exposure from BSs and active uplink users is given by*

$$F_{EI_a,\{1,2\}}(w) = \frac{1}{2} - \frac{1}{2j\pi} \int_0^\infty \int_0^\infty \frac{1}{t} [\exp(-jtw) \mathcal{L}_{EI_a}(-jt, r) - \exp(jtw) \mathcal{L}_{EI_a}(jt, r)] f_{R_u}''(r) dr dt,$$

in which $f_{R_u}''(r) = f_{R_u}(r)$ in the case of Scenario 1 and $f_{R_u}''(r) = f_{R_u}'(r)$ in the case of Scenario 2,

$$\begin{aligned} \mathcal{L}_{EI_a,\{1,2\}}(s, R_u') &= \mathcal{L}_{\{W_{b,a}, W_{b,a}'\}}(s \text{ SAR}_{dl}, R_u') \\ &\times \mathcal{L}_{W_{u,a,\{1,2\}}}(s \text{ SAR}_{dl}) \exp\left(-s \text{ SAR}_{ul} \max(p_{\max}, \rho_u R_u'^{\alpha\eta})\right) \\ &\times \left(\frac{1}{1+s \text{ SAR}_{dl} \rho_b G_b R_u'^{-\beta} (4\pi)^{-1}}\right), \\ \mathcal{L}_{W_{b,a}'}(s, R_u') &= \mathcal{L}_{W_{b,a}}(s \text{ SAR}_{dl}, R_u') \exp\left(-s \text{ SAR}_{dl} \frac{\rho_b G_b}{4\pi} R_u'^{-\beta}\right). \end{aligned} \quad (30)$$

The mean of the total passive exposure, including exposure from BSs and active uplink users is given by

$$\begin{aligned} \bar{E}I_a,\{1,2\} &= \int_0^\infty \left(\text{SAR}_{dl} G_b \rho_b (4\pi)^{-1} \left(r^{-\beta} + \frac{2\pi\lambda_b G_b}{\beta-2} r^{2-\beta} \right) \right. \\ &+ \text{SAR}_{ul} \min(p_{\max}, \rho_u r^{\alpha\eta}) \Big) f_{R_u}''(r) dr + \text{SAR}_{dl} \{\bar{p}_{u,p}, \bar{p}_{u,m}\} \\ &\times \frac{\lambda_c p_a \lambda_{cu} \pi r_c^2}{2} \int_0^\infty \int_0^{r_c+r_1} r^{-\beta} f_{R_2}(r|R_u) dr r_1 dr_1 \\ &+ \frac{\text{SAR}_{dl} \{\bar{p}_{u,p}, \bar{p}_{u,m}\}}{4\pi} \int_0^{r_c} \bar{m} \int_0^{r_c+r_1} r^{-\beta} f_{R_2}(r|R_u) dr \frac{2r_1}{r_c^2} dr_1, \end{aligned} \quad (31)$$

in which $\bar{m} = \frac{1}{m} \exp(-m + 1/m) - \exp(-m + 1/m) + \exp(-m)$, in which $m = p_a \lambda_{cu} \pi r_c^2$, is the average number of active users except the active user in the active user's cluster.

Proof: Follows the same lines as the proof of Theorem 2, thus omitted here. ■

V. COVERAGE PROBABILITY

In this section, we provide the analysis of the uplink coverage probability. At each resource block, there is only

one active user in the PV cell formed by BSs (while all the active uplink users contribute to the EMF exposure, only one user in each PV cell contributes to the interference of uplink transmission) or in the user cluster that the BS serves. Recall that we study the uplink coverage probability at the tagged BS, the BS that serves the active user. Let R_i be the distance from an interfering uplink user to its serving BS, which should be strictly less than the distance from this uplink user to the tagged BS, D , since the user associates with the nearest BS.

Lemma 9 (Distribution of the Distance between an Interfering Uplink User and its Associated BS R_i). *The PDF of R_i is given in [36], as*

$$f_{R_i}(r|D) = \frac{2\pi\lambda_b r \exp(-\lambda_b \pi r^2)}{1 - \exp(-\lambda_b \pi D^2)}, \quad 0 \leq r \leq D. \quad (32)$$

The density of uplink interferers observed from the tagged BS is well approximated by a non-homogeneous PPP with density $\lambda_b(1 - \exp(-\pi\lambda_b d^2))$ [43], in which d denotes the distance between a user to the tagged BS.

Lemma 10 (Laplace Transform of Interference and Noise). *The Laplace transform of the interference and noise is given by*

$$\begin{aligned} \mathcal{L}_{I_1+\sigma^2}(s) &= \exp(-s\sigma^2) \exp\left(-\lambda_b \int_0^\infty \int_0^x \frac{2\pi r \lambda_b \exp(-\lambda_b \pi r^2)}{1+s^{-1} \max(p_{\max}^{-1}, \rho_u^{-1} r^{-\alpha\eta}) x^\alpha G_b^{-1}} dr dx\right), \\ \mathcal{L}_{I_2+\sigma^2}(s) &= \exp(-s\sigma^2) \exp\left(-\lambda_b \int_0^\infty \int_0^{r_c} \frac{2r}{r_c^2} \left[1 - \frac{1}{1+s \min(p_{\max}, \rho_u r^{\alpha\eta}) x^{-\alpha} G_b}\right] dr dx\right). \end{aligned} \quad (33)$$

in which $\mathcal{L}_{I_1+\sigma^2}(s)$ is the Laplace transform of PPP user model and MCP user model Scenario 1, and $\mathcal{L}_{I_2+\sigma^2}(s)$ is the Laplace transform of Scenario 2 in the case of MCP user model.

Proof: Similar to [43], thus omitted here. ■

Finally, the uplink coverage probability is given in the following theorem.

Theorem 5 (Uplink Coverage Probability). *Uplink coverage of PPP user model and MCP user model Scenario 1, is given by*

$$P_{\text{cov}} = \int_0^\infty f_{R_u}(r) \mathcal{L}_{I_1+\sigma^2}(\gamma \max(p_{\max}^{-1}, \rho_u^{-1} r^{-\alpha\eta}) r^\alpha) dr, \quad (34)$$

and the uplink coverage probability of Scenario 2 in the case of MCP user model is given by,

$$P_{\text{cov},2} = \int_0^{r_c} \frac{2r}{r_c^2} \mathcal{L}_{I_2+\sigma^2}(\gamma \max(p_{\max}^{-1}, \rho_u^{-1} r^{-\alpha\eta}) r^\alpha) dr. \quad (35)$$

Proof: Uplink coverage probability is given by

$$\begin{aligned} P_{\text{cov}} &= \mathbb{P}(\text{SINR} > \gamma) = \mathbb{P}\left(G_b p_u H R_u^{-\alpha} > \gamma(I + \sigma^2)\right) \\ &= \mathbb{E}[\exp(-G_b^{-1} (I + \sigma^2) \gamma p_u^{-1} R_u^\alpha)], \end{aligned} \quad (36)$$

proof completes by taking the expectation over R_u , while in the PPP user model and Scenario 1 of MCP user model R_u

TABLE II
TABLE OF PARAMETERS

Parameter	Symbol	Simulation Value
Density of BSs	λ_b	1 BS/km ²
Density of user clusters	λ_c	1 BS/km ²
Antenna gain	G_b	10 dBi
Frequency	$f_{\{u,b\}}$	2600 MHz
Power control parameters	$\rho_{\{u,b\}}$	0.008 mW, 10 W
Maximum transmission power	p_{max}	200 mW
User cluster radius	r_c	100 m
Active probability	p_a	1
Noise power	σ^2	10^{-12} W
SINR threshold	γ	20 dB
path-loss parameters	α, β	4, 2.5
SAR reduced in uplink/downlink	SAR_{ul}, SAR_{dl}	$0.0053 \frac{W}{kg/W}, 0.0042 \frac{W}{kg/W}$ [44]

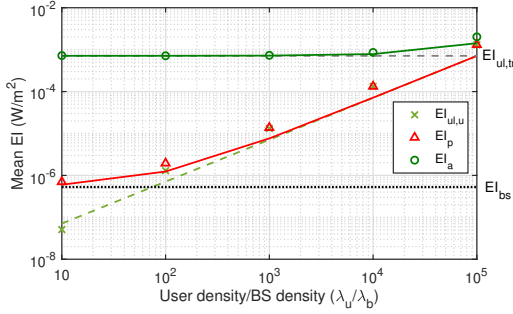


Fig. 3. The impact of user density on the mean EI and its different components: uplink users $EI_{ul,u}$, BSs EI_{bs} , and self-exposure from uplink transmission $EI_{ul,tr}$ (only a component of active users' EI, EI_a), for the PPP user model with $\eta = 0.4$.

is the first contact distance of PPP, and in Scenario 2 of MCP user model R_u is the distance to the cluster center. ■

VI. NUMERICAL RESULTS

Unless stated otherwise, we use the simulation parameters as listed in Table II. In all the provided figures, we use markers for simulations and lines for analytical results. Recall that EI_a and EI_p , as well as their different components, are defined in Definition, 6 (6) and (7).

In Fig. 3, we plot the mean of EI of the passive user (EI_p) and the active user (EI_a), respectively. Besides, we also plot the mean of EI from (i) BSs (EI_{bs}), (ii) self-exposure from uplink transmission ($EI_{ul,tr}$), and (iii) uplink transmission of other active uplink users ($EI_{ul,u}$). We show that when the ratio

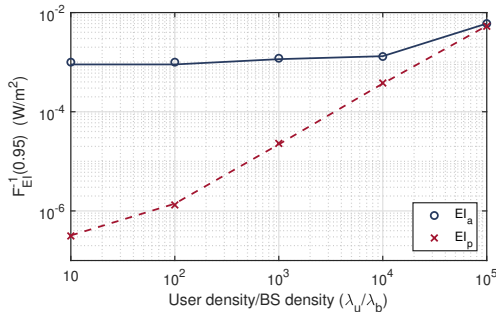


Fig. 4. The 95-th-percentile of EI for passive and active users under different user density to BS density ratios with $\eta = 0.4$.

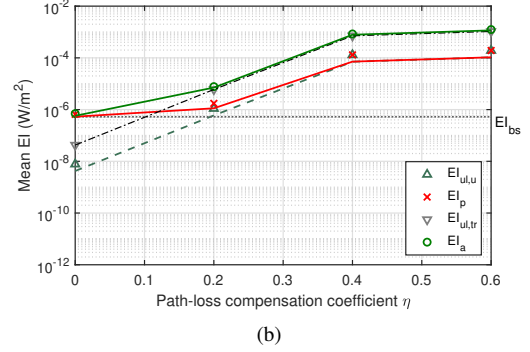
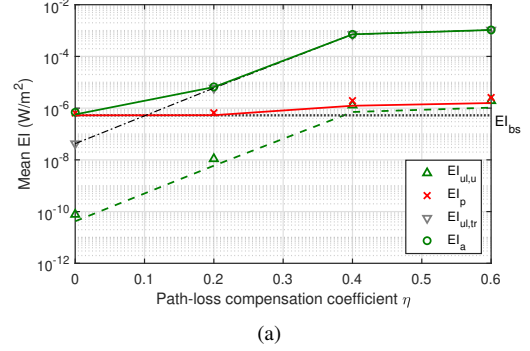


Fig. 5. Mean of EI of the active user EI_a and passive user EI_p , and their different components: uplink users $EI_{ul,u}$, BSs EI_{bs} , and self-exposure from uplink transmission $EI_{ul,tr}$, for different η at a fixed user density to BS density ratio for PPP user model (a) $\lambda_u/\lambda_b = 100$, and (b) $\lambda_u/\lambda_b = 10^4$.

of active uplink user density to the BS density (λ_u/λ_b) is low, the dominant EMF exposure of the passive user and the active user comes from BSs and uplink transmission of the user itself, respectively. With the increase of the ratio λ_u/λ_b , the EMF exposure from active uplink users increases and becomes of non-negligible magnitude, which is the intersection point in Fig. 3) compared to the EMF exposure from BSs starting from $\lambda_u/\lambda_b = 100$, and non-negligible compared to uplink transmission of an active user starting from $\lambda_u/\lambda_b = 10^5$, respectively.

In Fig. 4, we plot the 95-th percentile of EI of the passive and active user, respectively. As the exposure in 5G networks is stochastic, this metric is essential to assess exposure performance in 5G networks where we need to limit it below some threshold. Similarly, we observe that the EMF exposure from other active uplink users becomes non-negligible at extremely high λ_u/λ_b , e.g., $\lambda_u/\lambda_b > 10^4$.

In Fig. 5, we plot the mean of EI under different uplink power control coefficients, η , for (a) a less crowded case with $\lambda_u/\lambda_b = 100$ and (b) an extreme case with $\lambda_u/\lambda_b = 10^4$. Note that in Fig. 5 when $\eta = 0$, this implies the case where there is no path-loss compensation and all users transmit at the minimum transmit power, ρ_u . In this case, the EMF exposure from BSs is much greater than that from the uplink transmission, either from the user itself or other active users. With the increase of η , the EMF exposure from uplink transmission increases dramatically at first and then increases slowly. This is due to the limitation of the transmit power. More precisely,

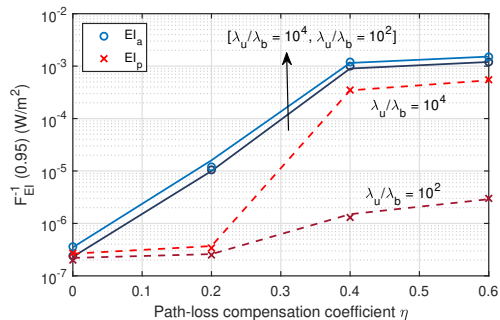


Fig. 6. The 95-th-percentile of EI for passive and active users under different η and at fixed user density to BS density ratio: $\lambda_u/\lambda_b = 100$ and $\lambda_u/\lambda_b = 10^4$.

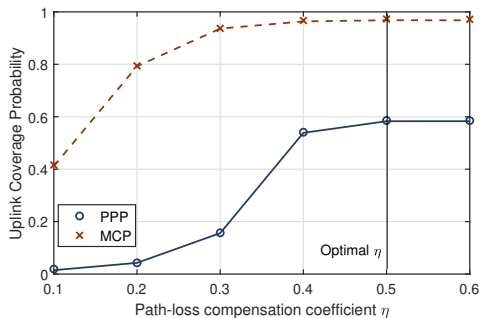


Fig. 7. Uplink coverage probability of PPP user model and MCP user model under different η .

when η increases from 0.2 to 0.4, almost all the active users' transmit power increases to p_{\max} . On the other hand, when η increases from 0.4 to 0.6, the transmit power of only a few active users (those located very close to the serving BS) increases to p_{\max} .

In the scenario of large user density to BS density ratio plotted in Fig. 5 (b), the mean of EI of the active user and passive user shows similar trends to the less crowded case plotted in Fig. 5 (a). Besides, we notice that comparing Fig. 5 (a) with Fig. 5 (b), while the mean of EI_p increases dramatically with the increase of λ_u/λ_b , the mean of EI_{bs} and $EI_{ul,tr}$ keep the same. Since $EI_{ul,tr}$ and EI_{bs} are not a function of user density, the average distance to the nearest BS and the average transmit power do not change with λ_u .

In Fig. 6, we show that at low values of η the passive user and the active user experience a similar level of EMF exposure which is mainly from BSs, and at high values of η the active user experiences a much higher level of EMF exposure because of its uplink transmission. With the increase of the user density to BS density ratio, the EMF exposure of the passive user increases dramatically while the exposure of the active user only changes slightly due to the fact that active exposure is much greater than passive exposure.

Fig. 7 shows the uplink coverage probability under different η for both PPP and MCP user models. We observe from the figure that there exists a value of η that maximizes the coverage probability for both user models. This is because the increase in the interference caused by increasing η becomes

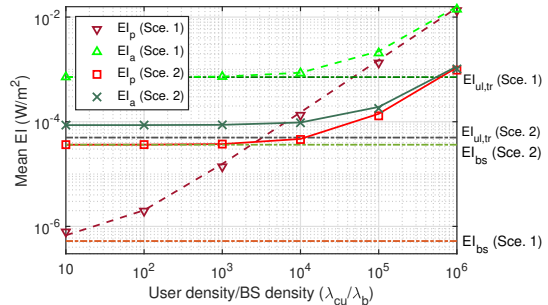


Fig. 8. The impact of user density to BS density ratio on the mean EI and its different components: BSs EI_{bs} and self-exposure from uplink transmission $EI_{ul,tr}$ (only a component of active users' EI), for the MCP user model with $\eta = 0.4$.

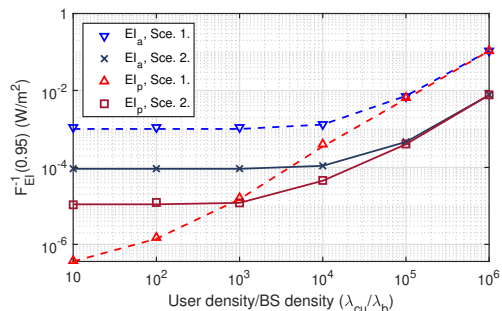


Fig. 9. The 95-th-percentile of EI for passive and active users for MCP user model in both scenarios, under different user density to BS density ratios and $\eta = 0.4$.

more significant than the increase in the quality of the uplink signal. Since we assume that BSs split the resources to serve the users to avoid intra-cell interference, uplink coverage probability is not a function of user densities, and it is only a function of η . With the increase of η , the transmit power increases, thus the coverage probability increases. However, EMF exposure to residents also increases. Therefore, there is a trade-off between good communication performance and EMF exposure.

In Fig. 8, we present the results for the mean of the EI in two different scenarios: Scenario 1, where user cluster centers are independently distributed according to a PPP, and Scenario 2, where user clusters are centered at the BSs. Interestingly, we observe that when the user density to BS density ratio (λ_{cu}/λ_b) is low, both passive and active users in Scenario 2 experience higher EMF exposure compared to Scenario 1.

In Fig. 9, we present the results for the 95-th percentile of the EI in the two aforementioned scenarios. We notice that in Scenario 1, the EMF exposure level increases gradually with the increase in λ_{cu}/λ_b . This finding suggests that when the density of users relative to the density of BSs is low, deploying BSs at the user cluster centers is not efficient. This is because, although placing a BS at the cluster center significantly reduces the transmit power of UE, it also increases exposure due to the high transmit power of the BS and the shorter distance between the BS and the users. However, if λ_{cu}/λ_b reaches 10^3 , deploying BSs at the user cluster centers becomes

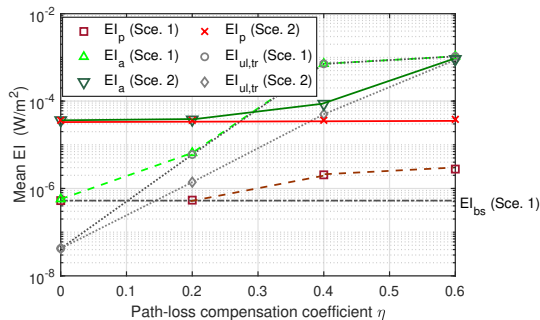


Fig. 10. The impact of user density on the mean EI and its different components: BSs EI_{bs} , and self-exposure from uplink transmission $EI_{ul,tr}$ (only a component of active users' EI), for the MCP user model under different η and $\lambda_{cu}/\lambda_b = 100$.

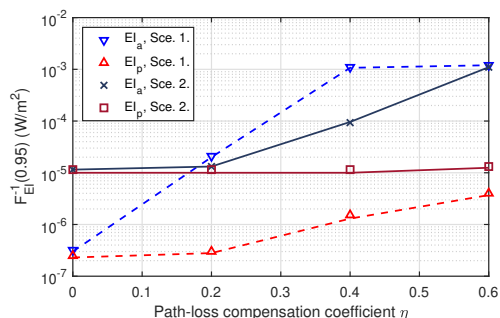


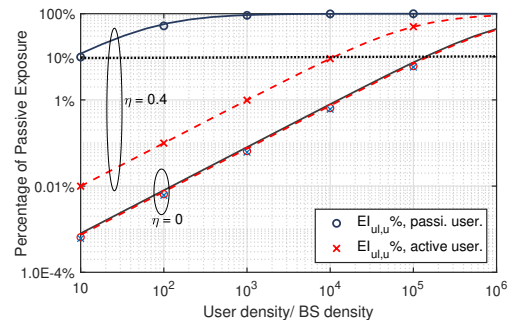
Fig. 11. The 95-th-percentile of EI for passive and active users for MCP user model in both scenarios under different η and $\lambda_{cu}/\lambda_b = 100$.

beneficial.

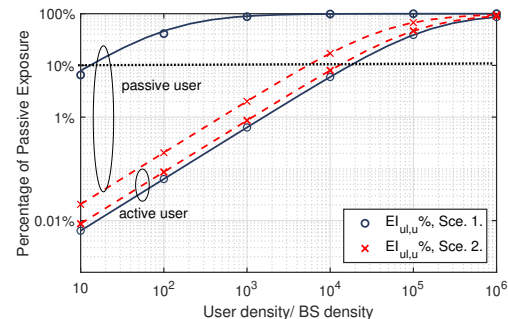
Fig. 10 shows the mean of EI under different η for MCP user model. $EI_{ul,tr}$ (Sc. 1) and $EI_{ul,tr}$ (Sc. 2) start at the same value when $\eta = 0$ since the active user has the same transmit power $p_o = \rho_u$ without path-loss compensation. As η increases, $EI_{ul,tr}$ (Sc. 1) becomes greater than $EI_{ul,tr}$ (Sc. 2). This is because the active user requires a higher transmit power to compensate for the path-loss when the BS is located further away in Scenario 1 compared to Scenario 2. However, as η continues to increase, $EI_{ul,tr}$ reaches its maximum achievable value, limited by the maximum transmit power of the devices.

In Fig. 11 we show the 95-th-percentile of EI under different η for MCP user model. We notice that while Scenario 1 is always beneficial for the passive user, it is only beneficial for the active users at low values of η .

To further show the impact of the passive EMF exposure, in Fig. 12, we plot the percentage of $EI_{ul,u}$ with respect to the total EMF exposure for both passive and active users, respectively. With the increase of the user density, the passive exposure from uplink users cannot be ignored if it contributes more than 10% of the total exposure (dotted line in Fig. 12): in PPP user case when $\eta = 0.4$, $EI_{ul,u}$ cannot be ignored when $\lambda_u/\lambda_b \geq 10$ for the passive user while $\lambda_u/\lambda_b \geq 10^4$ for the active user. Interestingly, we notice that in MCP case, $EI_{ul,u}$ has a higher impact on the active user when BSs are deployed at the cluster center compared to independent distribution. Even though deploying one BS at the cluster center reduces the $EI_{ul,u}$, the overall exposure reduces in both active exposure



(a)



(b)

Fig. 12. (a) Percentage of $EI_{ul,u}$ to the total exposure in PPP user model and (b) Percentage of $EI_{ul,u}$ to the total exposure in MCP user model.

and $EI_{ul,u}$. Thus, $EI_{ul,u}$ of Sc. 2 contributes more to overall exposure than in Sc. 1.

VII. CONCLUSION

In this study, we introduced a novel stochastic geometry framework to analyze the EMF exposure experienced by both passive and active users in cellular network. Unlike conventional approaches that neglect the EMF exposure from other uplink users, our analysis accounted for this crucial aspect, leading to more accurate and realistic results. We showed that passive exposure (exposure from uplink transmission of other users) accounts for more than 10% of the total exposure of the passive user even when the ratio between the user density and the BS density is as low as 10 users per BS. On the other hand, for active users, passive exposure starts to exceed 10% of the total exposure when the user density to the BS density ratio exceeds 10^4 users per BS. This research contributes to the understanding of EMF exposure in wireless networks and highlights the importance of considering interactions between users in the EMF exposure assessment.

APPENDIX

A. Proof of Lemma 7

In the case of the MCP user model, assuming the typical user is located at the origin. Therefore, we are conditioning on a typical cluster containing the origin, and the Laplace transform of W_u of a typical user is given by

$$\mathcal{L}_{W_u}(s) = \mathbb{E}_{W_u} \left[\exp \left(-s \sum_{x_{u,ij} \in \Phi_{cu}'} \frac{p_{u,x_{u,ij}} H_{x_{u,ij}} \|x_{u,ij}\|^{-\beta}}{4\pi} \right) \right]$$

$$\begin{aligned}
&\stackrel{(a)}{\approx} \mathbb{E}_{\Phi_c, p_u} \left[\prod_{c_i \in \Phi_c} \sum_{n=0}^{\infty} \frac{\exp(-\lambda_{cu} \pi r_c^2) (\lambda_{cu} \pi r_c^2)^n}{n!} \left(\int_0^{r_c + \|c_i\|} \frac{f_{R_2}(r \|c_i\|)}{1 + sp_u (4\pi)^{-1} r^{-\beta}} dr \right)^n \right] \mathbb{E}_{R_u, p_u} \left[\sum_{n=0}^{\infty} \frac{\exp(-\lambda_{cu} \pi r_c^2) (\lambda_{cu} \pi r_c^2)^n}{n!} \right. \\
&\quad \left. \times \left(\int_0^{r_c + R_u} \frac{f_{R_2}(r | R_u)}{1 + sp_u (4\pi)^{-1} r^{-\beta}} dr \right)^n \right] \\
&\stackrel{(b)}{=} \mathbb{E}_{\Phi_c, p_u} \left[\prod_{c_i \in \Phi_c} \exp \left(-\lambda_{cu} \pi r_c^2 \left(1 - \int_0^{r_c + \|c_i\|} \frac{f_{R_2}(r \|c_i\|)}{1 + sp_u (4\pi)^{-1} r^{-\beta}} dr \right) \right) \right] \mathbb{E}_{R_u, p_u} \left[\exp \left(-\lambda_{cu} \pi r_c^2 \left(1 - \int_0^{r_c + R_u} \frac{f_{R_2}(r | R_u)}{1 + sp_u (4\pi)^{-1} r^{-\beta}} dr \right) \right) \right], \quad (37)
\end{aligned}$$

in which the approximate sign comes from the assumption that users in one cluster have the same transmit power, step (a) follows computing the inter-cluster EMF and intra-cluster EMF separately, using the MGF of exponential random variables, computing the parent process and offspring process separately, and the i.i.d. property of each cluster and the number of active uplink users is a Poisson random variable $m \sim \text{Exp}(\lambda_{cu} \pi r_c^2)$, and (b) follows from the Taylor expansion of an exponential function.

Recall that we assume users in one cluster have the same transmit power in scenario 1, therefore, p_u is a function of the distance from the cluster center to the nearest BS, and given by

$$\begin{aligned}
\mathcal{L}_{W_{u,1}}(s) &= \mathbb{E}_{\Phi_c} \left[\prod_{c_i \in \Phi_c} \int_0^{\infty} \exp \left(-\lambda_{cu} \pi r_c^2 \left(1 - \int_0^{r_c + \|c_i\|} \frac{f_{R_2}(r \|c_i\|)}{1 + sp(z) (4\pi)^{-1} r^{-\beta}} dr \right) \right) f_{R_u}(z) dz \right] \mathbb{E}_{R_u} \left[\int_0^{\infty} \exp \left(-\lambda_{cu} \pi r_c^2 \left(1 - \int_0^{r_c + R_u} \frac{f_{R_2}(r | R_u)}{1 + sp(z) (4\pi)^{-1} r^{-\beta}} dr \right) \right) f_{R_u}(z) dz \right], \quad (38)
\end{aligned}$$

recall that $p(z) = \min(p_{\max}, \rho_u z^{\eta\alpha})$ and proof completes by using the PGFL of PPP and taking the expectation over R_u . In scenario 2, user clusters are centered at the BS, hence, the transmit power of users is a constant.

$$\begin{aligned}
\mathcal{L}_{W_{u,2}}(s) &= \mathbb{E}_{\Phi_c} \left[\prod_{c_i \in \Phi_c} \exp \left(-\lambda_{cu} \pi r_c^2 \left(1 - \int_0^{r_c + \|c_i\|} \frac{f_{R_2}(r \|c_i\|)}{1 + s\bar{p}_{u,m} (4\pi)^{-1} r^{-\beta}} dr \right) \right) \right] \mathbb{E}_{R_u} \left[\exp \left(-\lambda_{cu} \pi r_c^2 \left(1 - \int_0^{r_c + R_u} \frac{f_{R_2}(r | R_u)}{1 + s\bar{p}_{u,m} (4\pi)^{-1} r^{-\beta}} dr \right) \right) \right], \quad (39)
\end{aligned}$$

recall that $\bar{p}_{u,m} = \int_0^{\infty} \min(p_{\max}, \rho_u z^{\eta\alpha}) \frac{2z}{r_c^2} dz$, and similarly to $\mathcal{L}_{W_{u,1}}(s)$, proof completes by using the PGFL of PPP and taking the expectation over R_u .

B. Proof of Lemma 8

Recall that as for the active user, while the expression of inter-cluster EMF exposure keeps the same as passive user case, the expression of the intra-cluster EMF exposure is slightly different since the number of active uplink user within the reference's user cluster is $n - 1$ (in which n is the total number of the active uplink user). Therefore, the Laplace transform of $W_{u,a}$ of the active user is given by

$$\mathcal{L}_{W_{u,a}}(s) = \mathbb{E}_{\Phi_c, p_u} \left[\prod_{c_i \in \Phi_c} \sum_{n=0}^{\infty} \frac{\exp(-\lambda_{cu} \pi r_c^2) (\lambda_{cu} \pi r_c^2)^n}{n!} \left(\int_0^{r_c + \|c_i\|} \frac{f_{R_2}(r \|c_i\|)}{1 + sp_{u,c_i} (4\pi)^{-1} r^{-\beta}} dr \right)^n \right] \mathbb{E}_{R_u, p_u} \left[\sum_{n=1}^{\infty} \frac{\exp(-\lambda_{cu} \pi r_c^2) (\lambda_{cu} \pi r_c^2)^n}{n!} \right. \\
\left. \times \left(\int_0^{r_c + R_u} \frac{f_{R_2}(r | R_u)}{1 + sp_{u,c_0} (4\pi)^{-1} r^{-\beta}} dr \right)^{n-1} \right], \quad (40)$$

$$\begin{aligned}
&\text{in the case of Scenario 1,} \\
\mathcal{L}_{W_{u,a,1}}(s) &= \mathbb{E}_{\Phi_c} \left[\prod_{c_i \in \Phi_c} \int_0^{\infty} \exp \left(-\lambda_{cu} \pi r_c^2 \left(1 - \int_0^{r_c + \|c_i\|} f_{R_u}(z) \frac{f_{R_2}(r \|c_i\|)}{1 + sp(z) (4\pi)^{-1} r^{-\beta}} dr \right) \right) dz \right] \mathbb{E}_{R_u} \left[\int_0^{\infty} \frac{\exp(-\lambda_{cu} \pi r_c^2)}{\int_0^{r_c + R_u} \frac{f_{R_2}(r | R_u)}{1 + sp(z) (4\pi)^{-1} r^{-\beta}} dr} \right. \\
&\quad \left. \left(\exp \left(\lambda_{cu} \pi r_c^2 \int_0^{r_c + R_u} \frac{f_{R_2}(r | R_u)}{1 + sp(z) (4\pi)^{-1} r^{-\beta}} dr \right) - 1 \right) f_{R_u}(z) dz \right], \quad (41)
\end{aligned}$$

in the case of Scenario 2,

$$\begin{aligned}
\mathcal{L}_{W_{u,a,2}}(s) &= \mathbb{E}_{\Phi_c} \left[\prod_{c_i \in \Phi_c} \exp \left(-\lambda_{cu} \pi r_c^2 \left(1 - \int_0^{r_c + \|c_i\|} \frac{f_{R_2}(r \|c_i\|)}{1 + s\bar{p}_{u,m} (4\pi)^{-1} r^{-\beta}} dr \right) \right) \right] \mathbb{E}_{R_u} \left[\frac{\exp(-\lambda_{cu} \pi r_c^2)}{\int_0^{r_c + R_u} \frac{f_{R_2}(r | R_u)}{1 + s\bar{p}_{u,m} (4\pi)^{-1} r^{-\beta}} dr} \right. \\
&\quad \left. \times \left(\exp \left(\lambda_{cu} \pi r_c^2 \int_0^{r_c + R_u} \frac{f_{R_2}(r | R_u)}{1 + s\bar{p}_{u,m} (4\pi)^{-1} r^{-\beta}} dr \right) - 1 \right) \right], \quad (42)
\end{aligned}$$

proof completes by using the PGFL of PPP and taking the expectation of R_u .

REFERENCES

- [1] J. G. Andrews, S. Buzzi, W. Choi, S. V. Hanly, A. Lozano, A. C. Soong, and J. C. Zhang, "What will 5G be?" *IEEE Journal on Selected Areas in Communications*, vol. 32, no. 6, pp. 1065–1082, 2014.
- [2] "World telecommunication/ICT development report 2010 - monitoring the WSIS targets," *ITU telecom*, available online: <http://handle.itu.int/11.1002/pub/803655cd-en>.
- [3] D. Tillekeratne, M. Wilson, and L. Purnell, "Renewable energy for mobile towers: opportunities for low- and middle-income countries," *Global System Mobile Association (GSMA), Tech. Rep., Sep.*, 2020.
- [4] L. Chiaraviglio, S. Turco, G. Bianchi, and N. Blefari-Melazzi, "Do dense 5G networks increase exposure to electromagnetic fields?[point of view]," *Proceedings of the IEEE*, vol. 109, no. 12, pp. 1880–1887, 2021.
- [5] K. ITU-T recommendation, "Guidance on complying with limits for human exposure to electromagnetic fields," 2004.
- [6] I. C. on Non-Ionizing Radiation Protection *et al.*, "Guidelines for limiting exposure to time-varying electric, magnetic, and electromagnetic fields (up to 300 GHz)," *Health physics*, vol. 74, no. 4, pp. 494–522, 1998.
- [7] U. F. C. Commission *et al.*, "Human exposure to radiofrequency electromagnetic fields and reassessment of FCC radiofrequency exposure limits and policies. a rule by the federal communications commission on 04/01/2020 published in: the federal register; 2020," 2020.
- [8] H. M. Madjar, "Human radio frequency exposure limits: An update of reference levels in Europe, USA, Canada, China, Japan and Korea," in *2016 International Symposium on Electromagnetic Compatibility - EMC EUROPE*, 2016, pp. 467–473.
- [9] K. R. Foster, M. C. Ziskin, Q. Balzano, and A. Hirata, "Thermal analysis of averaging times in radio-frequency exposure limits above 1 GHz," *IEEE Access*, vol. 6, pp. 74 536–74 546, 2018.
- [10] D. Belpomme, L. Hardell, I. Belyaev, E. Burgio, and D. O. Carpenter, "Thermal and non-thermal health effects of low intensity non-ionizing radiation: An international perspective," *Environmental pollution*, vol. 242, pp. 643–658, 2018.
- [11] Y. A. Sambo, F. Heliot, and M. A. Imran, "A survey and tutorial of electromagnetic radiation and reduction in mobile communication systems," *IEEE Communications Surveys & Tutorials*, vol. 17, no. 2, pp. 790–802, 2014.

- [12] N. Leitgeb, A. Auvinen, H. Danker-hopfe, and K. S. Mild, "Potential health effects of exposure to electromagnetic fields (EMF)," *Scientific Committee on Emerging and Newly Identified Health Risks SCENIHR Opinion on Potential health*, vol. 10, p. 75635, 2016.
- [13] L. Chiaraviglio, A. Elzanaty, and M.-S. Alouini, "Health risks associated with 5G exposure: A view from the communications engineering perspective," *IEEE Open Journal of the Communications Society*, vol. 2, pp. 2131–2179, 2021.
- [14] S. Kim and I. Nasim, "Human electromagnetic field exposure in 5G at 28 GHz," *IEEE Consumer Electronics Magazine*, vol. 9, no. 6, pp. 41–48, 2020.
- [15] L. Chiaraviglio, C. Lodovisi, D. Franci, S. Pavoncello, T. Aureli, N. Blefari-Melazzi, and M.-S. Alouini, "Massive measurements of 5G exposure in a town: Methodology and results," *IEEE Open Journal of the Communications Society*, vol. 2, pp. 2029–2048, 2021.
- [16] S. Aerts, L. Verloock, M. Van Den Bossche, D. Colombi, L. Martens, C. Törnevik, and W. Joseph, "In-situ measurement methodology for the assessment of 5G NR massive MIMO base station exposure at sub-6 GHz frequencies," *IEEE Access*, vol. 7, pp. 184 658–184 667, 2019.
- [17] D. Colombi, P. Joshi, B. Xu, F. Ghasemifard, V. Narasaraju, and C. Törnevik, "Analysis of the actual power and EMF exposure from base stations in a commercial 5G network," *Applied Sciences*, vol. 10, no. 15, p. 5280, 2020.
- [18] C. Carciofi, A. Garzia, S. Valbonesi, A. Gandolfo, and R. Franchelli, "RF electromagnetic field levels extensive geographical monitoring in 5G scenarios: Dynamic and standard measurements comparison," in *2020 International Conference on Technology and Entrepreneurship (ICTE)*. IEEE, 2020, pp. 1–6.
- [19] Y. A. Sambo, M. Al-Imari, F. Héliot, and M. A. Imran, "Electromagnetic emission-aware schedulers for the uplink of OFDM wireless communication systems," *IEEE Transactions on Vehicular Technology*, vol. 66, no. 2, pp. 1313–1323, 2016.
- [20] H. Jiang, L. You, A. Elzanaty, J. Wang, W. Wang, X. Gao, and M.-S. Alouini, "Rate-splitting multiple access for uplink massive MIMO with electromagnetic exposure constraints," *IEEE Journal on Selected Areas in Communications*, 2023.
- [21] H. Ibraiwish, A. Elzanaty, Y. H. Al-Badarnah, and M.-S. Alouini, "EMF-aware cellular networks in RIS-assisted environments," *IEEE Communications Letters*, vol. 26, no. 1, pp. 123–127, 2021.
- [22] A. Subhash, A. Kammoun, A. Elzanaty, S. Kalyani, Y. H. Al-Badarnah, and M.-S. Alouini, "Optimal phase shift design for fair allocation in RIS aided uplink network using statistical CSI," *IEEE Journal on Selected Areas in Communications*, 2023, to appear.
- [23] B. Thors, A. Furuskär, D. Colombi, and C. Törnevik, "Time-averaged realistic maximum power levels for the assessment of radio frequency exposure for 5G radio base stations using massive MIMO," *IEEE Access*, vol. 5, pp. 19 711–19 719, 2017.
- [24] P. Baracca, A. Weber, T. Wild, and C. Grangeat, "A statistical approach for RF exposure compliance boundary assessment in massive MIMO systems," in *WSA 2018; 22nd International ITG Workshop on Smart Antennas*. VDE, 2018, pp. 1–6.
- [25] L. Chiaraviglio, S. Rossetti, S. Saida, S. Bartoletti, and N. Blefari-Melazzi, "'Pencil beamforming increases human exposure to electromagnetic fields': True or false?" *IEEE Access*, vol. 9, pp. 25 158–25 171, 2021.
- [26] L. Chiaraviglio, C. Lodovisi, S. Bartoletti, A. Elzanaty, and M. Slim-Alouini, "Dominance of smartphone exposure in 5G mobile networks," *IEEE Transactions on Mobile Computing*, 2023.
- [27] L. Chiaraviglio, A. S. Cacciapuoti, G. Di Martino, M. Fiore, M. Montesano, D. Trucchi, and N. B. Melazzi, "Planning 5G networks under EMF constraints: State of the art and vision," *IEEE Access*, vol. 6, pp. 51 021–51 037, 2018.
- [28] Q. Gontier, L. Petrillo, F. Rottenberg, F. Horlin, J. Wiart, C. Oestges, and P. De Doncker, "A stochastic geometry approach to EMF exposure modeling," *IEEE Access*, vol. 9, pp. 91 777–91 787, 2021.
- [29] C. Wiame, S. Demey, L. Vandendorpe, P. De Doncker, and C. Oestges, "Joint data rate and EMF exposure analysis in Manhattan environments: stochastic geometry and ray tracing approaches," *arXiv preprint arXiv:2301.11097*, 2023.
- [30] Q. Gontier, C. Wiame, S. Wang, M. Di Renzo, J. Wiart, F. Horlin, C. Tsigros, C. Oestges, and P. De Doncker, "Joint metrics for EMF exposure and coverage in real-world homogeneous and inhomogeneous cellular networks," *Available online: <https://arxiv.org/abs/2302.03559>*, 2023.
- [31] N. A. Muhammad, N. Seman, N. I. A. Apandi, C. T. Han, Y. Li, and O. Elijah, "Stochastic geometry analysis of electromagnetic field exposure in coexisting sub-6 GHz and millimeter wave networks," *IEEE Access*, vol. 9, pp. 112 780–112 791, 2021.
- [32] L. Chen, A. Elzanaty, M. A. Kishk, L. Chiaraviglio, and M.-S. Alouini, "Joint uplink and downlink EMF exposure: Performance analysis and design insights," *IEEE Transactions on Wireless Communications*, 2023, to appear.
- [33] Y. Qin, M. A. Kishk, and M.-S. Alouini, "Performance evaluation of UAV-enabled cellular networks with battery-limited drones," *IEEE Communications Letters*, vol. 24, no. 12, pp. 2664–2668, 2020.
- [34] M. Afshang, C. Saha, and H. S. Dhillon, "Nearest-neighbor and contact distance distributions for Matérn cluster process," *IEEE Communications Letters*, vol. 21, no. 12, pp. 2686–2689, 2017.
- [35] Y. Qin, M. A. Kishk, and M.-S. Alouini, "Energy efficiency analysis of charging pads-powered UAV-enabled wireless networks," *IEEE Transactions on Wireless Communications*, vol. 22, no. 7, pp. 4683–4697, 2023.
- [36] M. Haenggi, *Stochastic geometry for wireless networks*. Cambridge University Press, 2012.
- [37] Y. Qin, M. A. Kishk, and M.-S. Alouini, "On the influence of charging stations spatial distribution on aerial wireless networks," *IEEE Transactions on Green Communications and Networking*, vol. 5, no. 3, pp. 1395–1409, 2021.
- [38] H. ElSawy and E. Hossain, "On stochastic geometry modeling of cellular uplink transmission with truncated channel inversion power control," *IEEE Transactions on Wireless Communications*, vol. 13, no. 8, pp. 4454–4469, 2014.
- [39] Y. Qin, M. A. Kishk, and M.-S. Alouini, "On the uplink SINR meta distribution of UAV-assisted wireless networks," *IEEE Wireless Communications Letters*, vol. 12, no. 4, pp. 684–688, 2023.
- [40] J. Gil-Pelaez, "Note on the inversion theorem," *Biometrika*, vol. 38, no. 3–4, pp. 481–482, 1951.
- [41] Y. Qin, M. A. Kishk, and M.-S. Alouini, "A dominant interferer plus mean field-based approximation for SINR meta distribution in wireless networks," *IEEE Transactions on Communications*, vol. 71, no. 6, pp. 3663–3678, 2023.
- [42] M. A. Kishk and H. S. Dhillon, "Joint uplink and downlink coverage analysis of cellular-based RF-powered IoT network," *IEEE Transactions on Green Communications and Networking*, vol. 2, no. 2, pp. 446–459, 2018.
- [43] S. Singh, X. Zhang, and J. G. Andrews, "Joint rate and SINR coverage analysis for decoupled uplink-downlink biased cell associations in Het-Nets," *IEEE Transactions on Wireless Communications*, vol. 14, no. 10, pp. 5360–5373, 2015.
- [44] G. Vermeeren, D. Plets, W. Joseph, L. Martens, C. Oliveira, D. Sebastiao, M. Ferreira, F. Cardoso, L. Correia, M. Koprivica *et al.*, "Low EMF exposure future networks D2. 8 global wireless exposure metric definition," *LEXNET Consortium, Moulinaux, France, Tech. Rep. D*, vol. 2, 2015.